# Energy Control System of Solar Powered Wheelchair

Yoshihiko Takahashi, Syogo Matsuo, and Kei Kawakami
*Department of Mechanical System Engineering*
*Department of Vehicle System Engineering*
*Kanagawa Institute of Technology*
*Japan*

## 1. Introduction

Independence is a major concern for individuals with severe handicaps. Welfare assistance robotic technology is a popular solution to this concern (e.g. Hashino, 1996; Takahashi, Ogawa, and Machida, 2002 and 2008). Assistance robotic technologies offer potential alternatives to the need for human helpers. People bound to wheelchairs have limited mobility reliant on battery life, which only allows for short distance travel between charges. In addition, recharging batteries is time consuming.

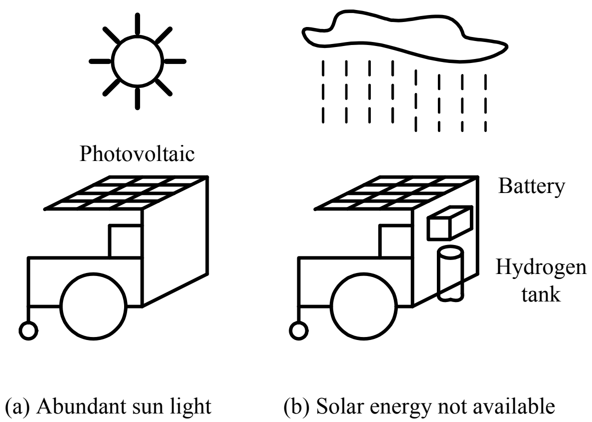


Fig. 1. Running conditions of proposed robotic wheelchair

The aim of this paper is to propose a system which will increase the moving distance of an electrical wheelchair by adding two solar powered energy sources; a small photovoltaic cell and a fuel cell. Fig.1 displays the running conditions of the proposed robotic wheelchair. The control system will ideally give priority to the photovoltaic cell, next to the fuel cell and finally to the battery. When sufficient sun light is available, the photovoltaic cell on the wheelchair roof is used, when it is limited, the fuel cell or the battery is used. The energy control system is designed using a micro computer, and the energy source is quickly

Source: Solar Energy, Book edited by: Radu D. Rugescu,
ISBN 978-953-307-052-0, pp. 432, February 2010, INTECH, Croatia, downloaded from SCIYO.COM

changeable. Our objective is that the proposed robotic solar wheelchair will enable users to enjoy increased independence when they are outdoors.
The advantage of using a solar powered energy source is that it produces power without requiring use of fossil fuels. A photovoltaic cell is installed on the roof of the wheelchair, which produces enough power to operate the apparatus when enough sun light is available. The battery is charged using a large photovoltaic cell on the roof of the setup. Hydrogen is produced using a water electrolysis hydrogen generator, and the fuel cell utilizes the produced hydrogen. The large photovoltaic cell also sends electricity to the hydrogen generator.
Photovoltaic cells and fuel cells are representative sustainable technologies (Bialasiewicz, 2008; Okabe et al., 2009; KE Jin et al., 2009). We are able to use two methods to produce hydrogen using these sustainable technologies for our wheelchair. The first method is to generate hydrogen from the electrolysis of water. The next is to use waste biomass which produces biomass ethanol. Hydrogen is produced by steam reforming the ethanol (Takahashi, & Mori, 2006; Essaki et al., 2008; Saxena et al., 2009; Rubin, 2008; Sugano, & Tamiya, 2009). Standard sized fuel cell models are developed with the aim to develop a commercially viable vehicle (Tabo et al., 2004; Kotz, et al., 2001; Rodatz, et al., 2001). Hybrid vehicles using photovoltaic cells and fuel cells are developed in two universities (Konishi, et al., 2008; Obara, 2004). Small fuel cell vehicles were developed (Nishimura, 2008; Takahashi, 2009a and 2009b). A wheelchair with a fuel cell has been developed (Yamamuro, 2003).
This paper will present a robotic wheelchair using solar powered energy sources of the photovoltaic and fuel cell, detail the energy flow concept for charging electricity to the battery and for storing hydrogen to the tank, the mechanical construction, the energy control system, and the experimental results of the running test.

## 2. Energy flow of proposed robotic wheelchair

A schematic explanation and block diagram of the energy flow used in the proposed robotic wheelchair are shown in Figs. 2 and 3. The energy system used in the robotic wheelchair does not exhaust carbon dioxide as it does not utilize fossil fuels.
The first energy flow line in the schematic diagrams is the line from the photovoltaic cells on the roof of the wheelchair. A cascade connection of two photovoltaic cells (Kyosera, KC-40TJ) of 17.4 V and 43 W in nominal value is utilized as the energy source. The output voltage is reduced to 24 V using a DC-DC converter.
The second energy line is the line from the water electrolysis hydrogen generator. The photovoltaic cell on the setup roof (approximately 10 kW) sends electricity to the water electrolysis hydrogen generator. The generated hydrogen is stored in a metal hydride hydrogen tank of 60 NL. The output pressure of the hydrogen generator is approximately 0.3 MPa. The hydrogen tanks are installed on the wheelchair body after storing hydrogen. A metal hydride tank is used for safety concerns. A fuel cell (Daido Metal, HFC-24100) producing 24 V and 100 W in nominal values is used to generate electricity to the motor.
The third energy flow line is the battery line. The battery is charged with electricity from the photovoltaic cell producing approximately 10 kW on the setup roof, and then installed on the wheelchair body.
The fourth energy flow line is the biomass line. Ethanol is produced from waste biomass. Hydrogen is then generated from the ethanol using a steam reforming hydrogen generator. The generated hydrogen is stored in a 60 NL metal hydride hydrogen tank. The hydrogen

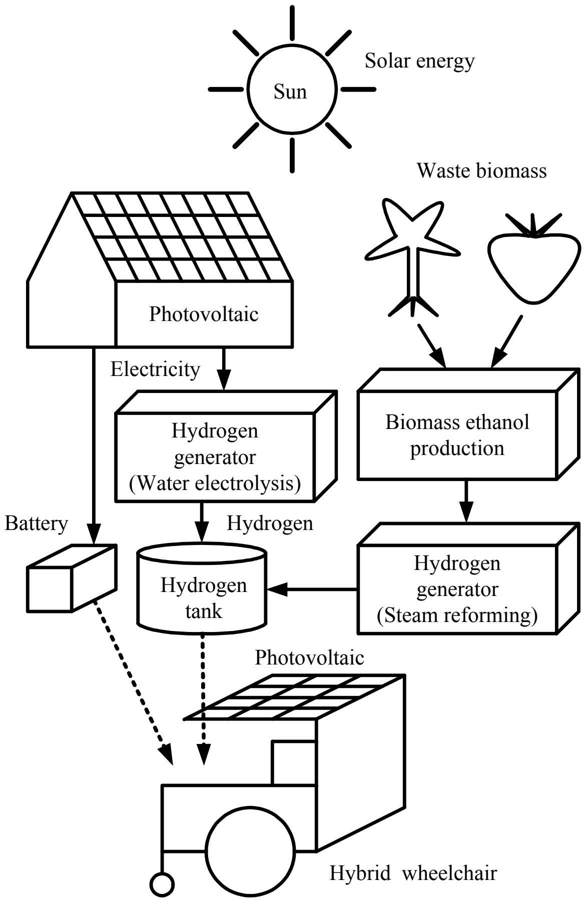


Fig. 2. Schematic explanation of energy flow

tanks are installed on the wheelchair body in the same manner as the second line. Ethanol is safe to handle, and is easy to carry, however, the fourth energy flow line is still a matter under consideration.

The High-Tech Research Center Project for Solar Energy System at the Kanagawa Institute of Technology is conducting research on applications of solar energy. The development of the robotic wheelchair is conducted as a part of the High-Tech Research Center Project. The battery charging and hydrogen storing to the metal hydride are conducted using the facility at the High-Tech Research Center Project.

## 3. Mechanical construction

Fig. 4 displays the fabricated robotic wheelchair with the photovoltaic and fuel cell. A reinforced YAMAHA JW-1 wheelchair was used as the main body of the experimental set up. In this configuration, the photovoltaic cell, the fuel cell, and the battery are installed on the top, on the back, and under the wheelchair, respectively. The energy control system and

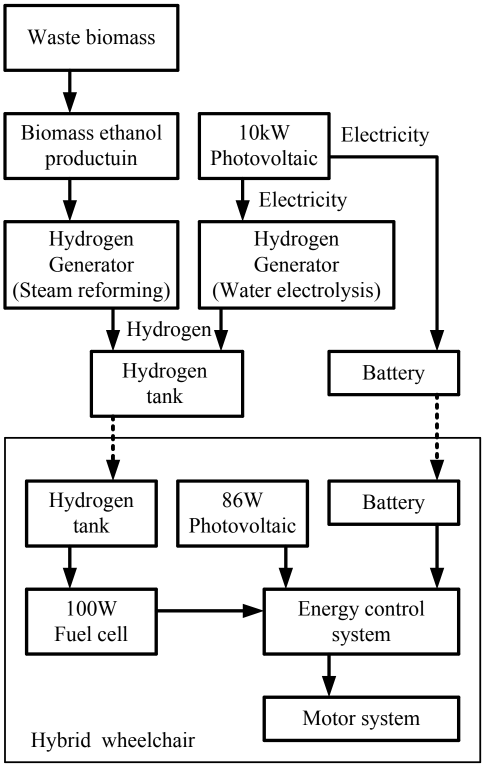


Fig. 3. Block diagram of energy flow

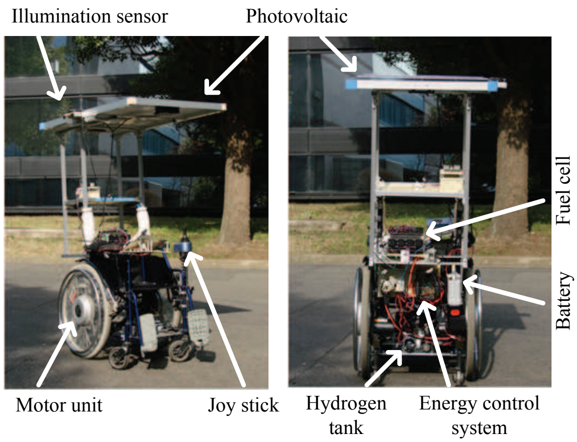


Fig. 4. Fabricated robotic wheelchair with photovoltaic and fuel cell

hydrogen tanks are installed on the back of the wheelchair. Figs.5 (a) and (b) show the photovoltaic and illumination sensor. Fig.6 (a) exhibits the fuel cell (Daido Metal, HFC-24100) and the vibration isolator. Fig.6 (b) shows the metal hydride tanks of 60 NL and 0.3

MPa. The hydrogen pressure is adjusted to 0.08 MPa using a regulator. The main specifications are as follows.

Wheelchair mechanism (Yamaha, JW-1)
 Weight : 13 kg
 Running operation : Joy stick
 Motor : DC24V, 90Wx2
Photovoltaic (Kyosera, KC-40TJ)
 Type : Multi crystal
 Nominal power : 43 W
 Maximum voltage : 17.4 V
 Dimensions : 526x652x54 mm
 Weight : 4.5 kg
Fuel cell (Daido Metal, HFC-24100)
 Nominal power : 100 W
 Nominal voltage : 24 V
 Dimensuions : 160x110x240 mm
 Weight : 3 kg
 Air fans : DC24, 0.94Wx 24

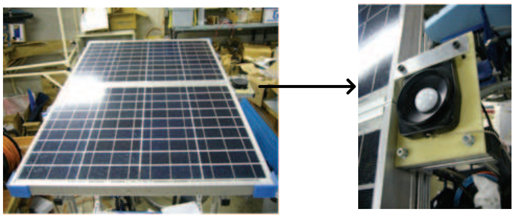

(a) Photovoltaic (b) Illumination sensor

Fig. 5. Photovoltaic and illumination sensor

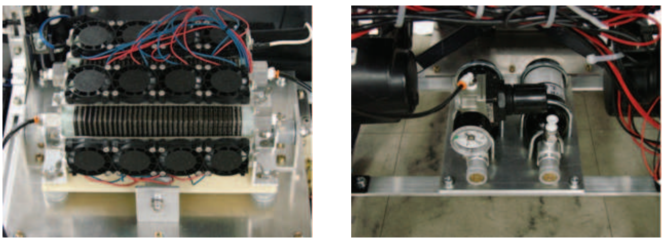

(a) Fuel cell and vibration isolator (b) Hydrogen tank and regulator

Fig. 6. Fuel cell and hydride tank

## 4. Energy control system

Fig.7 shows the concept of the energy control system where a micro computer determines the wheelchair condition, and selects the optimum energy source from the three energy sources: the photovoltaic on the wheelchair roof; the fuel cell; or the battery. Solid lines indicate energy flow lines, and dotted lines indicate the control signal flow lines. Fig.8 displays energy control architecture in detail. The switching control system inputs the voltages of the photovoltaic cell, the fuel cell, and the motor drive current, and selects the energy source determined by the wheelchair condition.

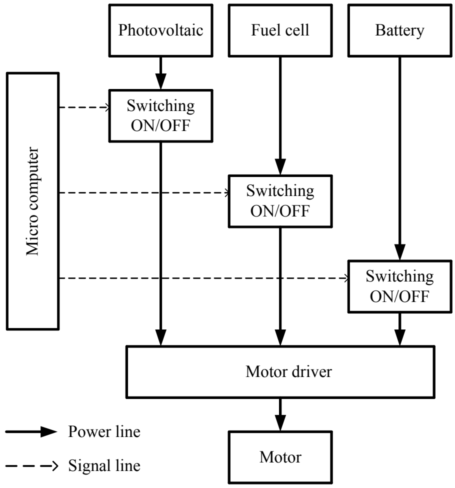


Fig. 7. Concept of energy control system

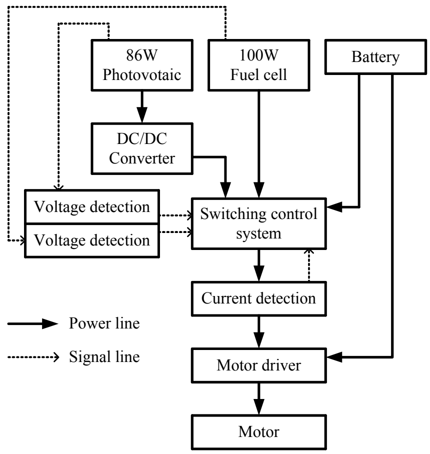


Fig. 8. Detailed energy control architecture

Fig.9 is the software control algorithm of the energy control system. Fig.10 shows the fabricated switching control system of the energy control system where a micro computer controls the entire energy control system, and FETs are used to switch the energy flow. Performance of energy source switching is also tested as this is the first attempt to develop a solar powered wheelchair. The electricity acquired from the photovoltaic cell on the wheelchair roof will be utilized to charge with the battery. Instant power increase using a capacitor will also be required. Improvement of the energy control system must be addressed in future research.

The control system will ideally give priority to the photovoltaic cell then to the fuel cell and then to the battery. Essentially, the switching control is conducted on the motor driving current considering the condition of the photovoltaic and fuel cells. If the motor driving current is below 2.5 A and the photovoltaic voltage is above 30 V, then the photovoltaic is selected. If the motor driving current is below 4.0 A and the fuel cell voltage is above 24 V, then the fuel cell is selected. When the motor driving current is below 20.0 A, then the battery is selected. The following details the software control algorithm of the energy control system.

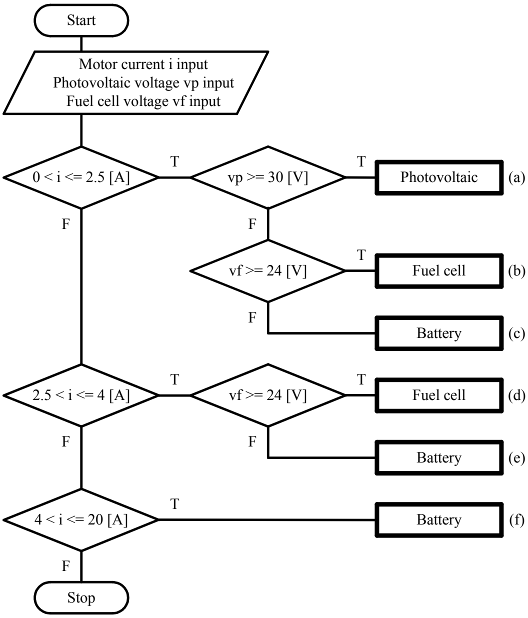


Fig. 9. Software control algorithm of energy control system

Condition (a) :

When the motor current is over 0.0 A and less than 2.5 A,
and the photovoltaic voltage is over 30 V,
then the photovoltaic is selected.

Condition (b) :

When the motor current is over 0.0 A and less than 2.5 A,
and the photovoltaic voltage is less than 30 V,
and the fuel cell voltage is over 24 V,
then the fuel cell is selected.

Condition (c) :

When the motor current is over 0.0 A and less than 2.5 A,
and the photovoltaic voltage is less than 30 V,
and the fuel cell voltage is less than 24 V,
then the battery is selected.

Condition (d) :
When the motor current is over 2.5 A and less than 4.0 A,
and the fuel cell voltage is over 24 V,
then the fuel cell is selected.

Condition (e) :
When the motor current is over 2.5 A and less than 4.0 A,
and the fuel cell voltage is less than 24 V,
then the battery is selected.

Condition (f) :
When the motor current is over 4.0 A and less than 20.0 A,
then the battery is selected.

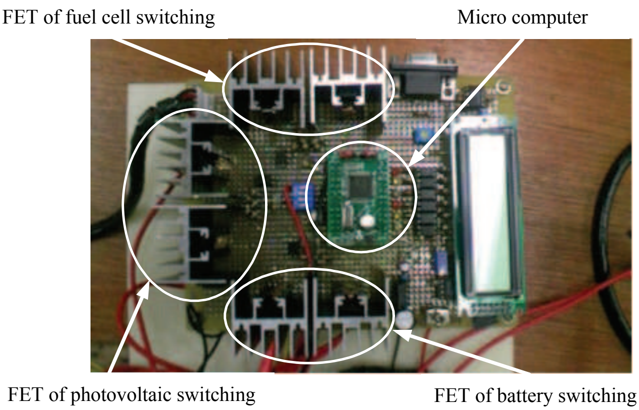


Fig. 10. Fabricated switching control system of energy control system

## 5. Experimental results

We conducted experiments on energy source selection between the solar panel, the fuel cell, and the battery.

### 5.1 Experimental conditions

The wheelchair was tested on a flat, straight course. It maintained the same speed maneuvering between two turning points during which joystick operation was required.
Figs.11 to 13 present the experimental results of the running tests using the fabricated wheelchair. Each figure will be detailed later. In each figure, the top graph shows the results of the motor driving current, the photovoltaic (PV) current, and the fuel cell (FC) current. Second, the results of the photovoltaic (PV) voltage, and the fuel cell (FC) voltage. The third figure from the top shows the results of the photovoltaic (PV) power and fuel cell (FC) power. Finally, the last chart shows illumination.
The following four test patterns are conducted;

1. Low Speed mode, Low (approximately 1.4 km/h) (Fig.11)
2. Low Speed mode, High (approximately 2.4 km/h) (Fig.12)
3. High Speed mode, Low (approximately 3.0 km/h) (Fig.13)

4. High Speed mode, High (approximately 3.4 km/h) (Fig.14)

Low Speed and High Speed modes are selected using a switch on the wheelchair frame. "Low" refers to the joy stick declined approximately 10 degrees, "High" refers to the joy stick declined completely. For example, the condition of the "Low Speed mode, Low" denotes that the switch was selected to low speed mode and the joy stick was inclined by approximately 10 degrees. The charts from Figs. 11 through 14 show the results of the conditions: Low Speed mode, Low; Low Speed mode, High; High Speed mode, Low; and High Speed mode, High, respectively.

### 5.2 Results of "Low Speed mode, Low" condition

Fig.11 (a) shows the experimental results of the current at the "Low Speed mode, Low" condition. The speed was approximately 1.4 km/h. The experimental results show that the average value of the motor driving current was approximately 1.5 A while moving straight on the course. The photovoltaic current was approximately the same value of the motor driving current. The fuel cell current was small. At the turning point, the motor driving current was over 2.5 A, therefore the current of the photovoltaic and fuel cell were lower than the required motor driving current. Energy from the battery was necessary.

Fig.11 (b) shows the experimental results of the voltage. While moving on the straight course, the photovoltaic voltage was reduced, and the fuel cell did not change greatly.

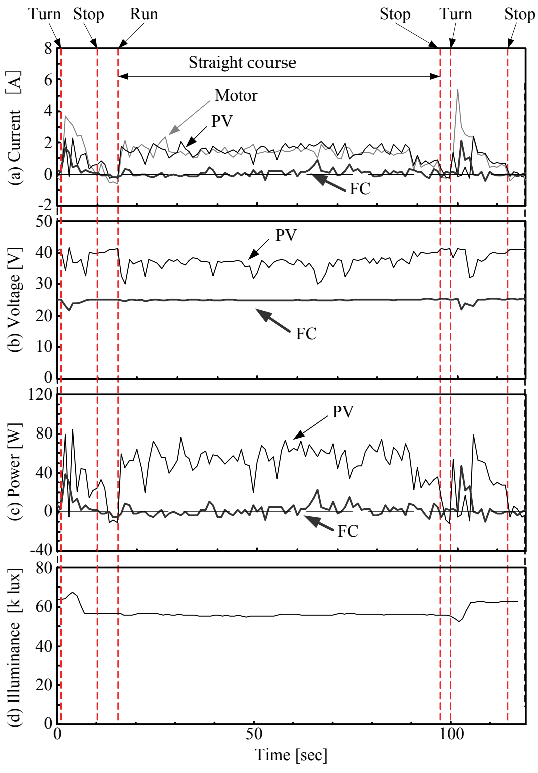


Fig. 11. Experimental results (Low Speed mode, Low)

Fig. 11 (c) shows the experimental results of the power. While moving on the straight course, the photovoltaic power was larger than the fuel cell power. Fig.11 (d) shows the experimental results of the illumination. Illumination was approximately 60 k lux while moving on the straight course. The illumination value changed while turning at the course ends.

### 5.3 Results of "Low Speed mode, High" condition

Fig.12 (a) shows the experimental results of the current at the "Low Speed mode, High" condition. The speed was approximately 2.4 km/h. The experimental results show that the average value of the motor driving current was approximately 1.8 A while moving on the straight portion of the course. The photovoltaic current was approximately the same value as the motor driving current. The photovoltaic current was occasionally reduced to 0 A. Fuel cell current was negligible. During turns, the motor driving current was over 4.0 A. The photovoltaic and fuel cell current were less than the motor driving current, therefore battery energy was required.

Fig.12 (b) shows the experimental results of the voltage. While moving on the straight part of the course, the photovoltaic voltage was lowered, the change in the fuel cell was negligible. Fig.12 (c) shows the experimental results of the power. The photovoltaic power

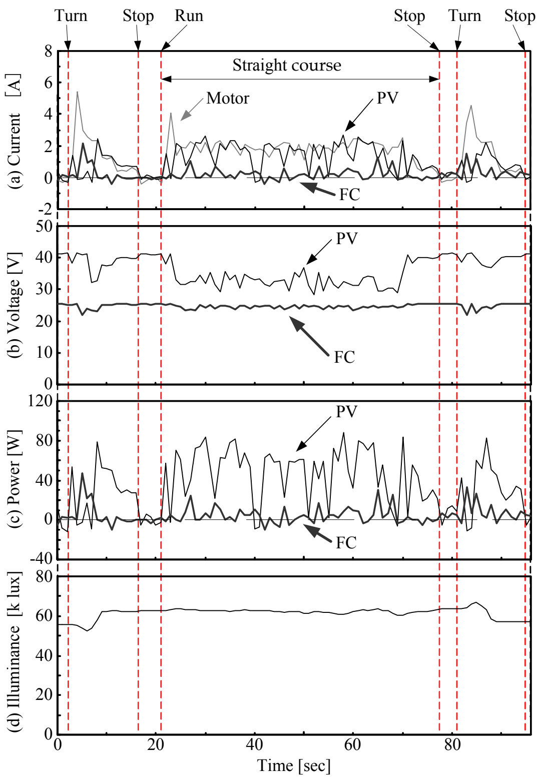


Fig. 12. Experimental results (Low Speed mode, High)

was larger than the fuel cell power. Fig.12 (d) shows the experimental results of the illumination. The illumination was approximately 60 k lux while moving on the straight part of the course. The illumination value changed while turning at the course ends.

### 5.4 Results of "High Speed mode, Low" condition

Fig.13 (a) shows the experimental results of the current at the "High Speed mode, Low" condition. The speed was approximately 3.0 km/h. The experimental results show that the average value of the motor driving current was approximately 2.0 A while moving straight. The photovoltaic current was approximately the same value as the motor driving current. The photovoltaic current occasionally fell to 0 A. Fuel cell current was minimal. At the turning point, the motor driving current was over 4.0 A, and the current of the photovoltaic and fuel cells were smaller than the motor driving current. Battery energy was required.

Fig.13 (b) shows the experimental results of the voltage. While moving straight, photovoltaic voltage decreased, and the fuel cell did not change prominently. Fig.13 (c) shows the experimental results of the power. While moving straight, photovoltaic power was larger than fuel cell power. Fig.13 (d) shows the experimental results of the illumination. Illumination was approximately 60 k lux while moving straight. It changed while turning at the course ends.

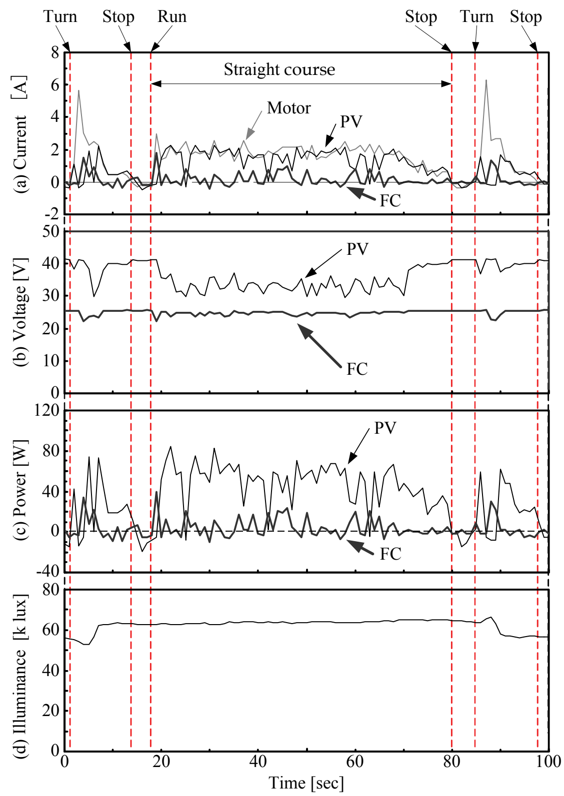


Fig. 13. Experimental results (High Speed mode, Low)

### 5.5 Results of "High Speed mode, High" condition

Fig.14 (a) shows the experimental results of the current at the "High Speed mode, High" condition. The speed was approximately 3.4 km/h. The experimental results show that the average value of the motor driving current was approximately 2.8 A while moving straight. Photovoltaic current was approximately 0 A. Fuel cell current increased, however the value was smaller than the motor driving current. Combined energy from the fuel cell and the battery was used. At the turning point, the motor driving current was over 4.0 A, and the current of the photovoltaic and fuel cell were smaller than the motor driving current. Energy from the battery was required.

Fig.14 (b) shows the experimental results of the voltage. While moving straight, the photovoltaic voltage was not reduced, however the fuel cell was. Fig.14 (c) shows the experimental results of the power. While moving the straight course, the photovoltaic power was not significant, and the fuel cell power increased. Fig.14 (d) shows the experimental results of the illumination. Illumination was approximately 60 k lux while moving straight. The illumination value changed while turning at the course ends.

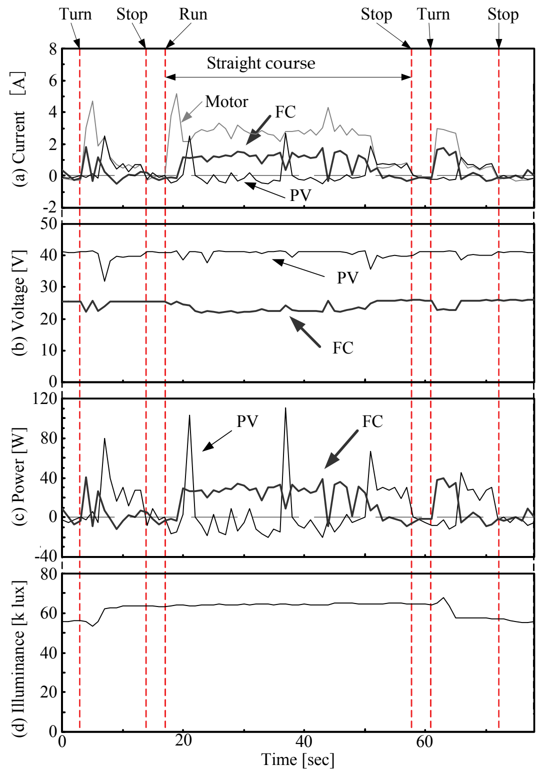


Fig. 14. Experimental results (High Speed mode, High)

### 5.6 Summary of the experimental results

The proposed robotic solar powered wheelchair uses a small powered photovoltaic of 86 W (at nominal value), and a small powered fuel cell of 100 W (at nominal value). When ample sun light is available, a flat and straight course is used, and the wheelchair travels at a low speed, the robotic wheelchair is able to move primarily powered by the photovoltaic cell. As a result, the solar powered wheelchair is able to travel further distances. When the wheelchair travels at higher speeds, and turns, it requires greater power, therefore it uses the energy from the fuel cell and the battery.

## 6. Conclusions

A new robotic solar powered wheelchair using three energy sources, a small photovoltaic cell, a small fuel cell, and a battery is proposed in this paper. All three energy sources use solar energy. The photovoltaic cell uses sun light directly. The battery is charged with electricity provided by the large photovoltaic cell installed on the setup roof. Hydrogen for the fuel cell is generated by a water electrolysis hydrogen generator, which is also powered by the same large photovoltaic cell on the building roof. The energy control system selects the optimal energy source to use based on various driving conditions.

It was confirmed from the experimental results that the robotic wheelchair is able to maneuver mainly using the photovoltaic cell when good moving conditions are available (i.e. abundant sun light, a flat and straight course, and low speed). The experimental results demonstrate that the robotic wheelchair is able to increase its moving distance. When moving conditions are not optimal, the robotic solar wheelchair uses energy from the fuel cell and the battery.

Improvements to the energy control system such as charging to the battery from the photovoltaic cell on the wheelchair roof, power increase using a capacitor, and hydrogen generation from waste biomass, must be addressed in future research.

## 7. Acknowledgments

The authors would like to express their deepest gratitude to the research staff of the High-Tech Research Center Project for Solar Energy Systems at the Kanagawa Institute of Technology for their kind cooperation with the experiments and for their kind advice.

## 8. References

Hashino, H. (1996); Daily Life Support Robot, *Journal of Robotics Society of Japan,* Vol.14, No.5, pp.614-618

Takahashi, Y., Ogawa, S., and Machida, S., (2002); Mechanical design and control system of robotic wheelchair with inverse pendulum control, Trans. Inst. Meas. Control, vol.24, no.5, pp.355-368.

Takahashi, Y., Ogawa, S., and Machida, S., (2008); Experiments on step climbing and simulations on inverse pendulum control using robotic wheelchair with inverse pendulum control, Trans. Inst. Meas. Control, vol.30, no.1, pp.47-61.

Takahashi, J., And Mori, T., (2006); Hydrogen Production from Reaction of Apple Pomace with Water over Commercial Stream Reforming Ni Catalysis, Journal of Japan Petroleum Institute, vol.49, no.5, pp.262-267.

Essaki, K., Muramatsu, T., and Kato, M., (2008); Hydrogen Production from Ethanol by Equilibrium Shifting Using Lithium Silicate Pellet as CO2 Absorbent, Journal of Japan Institute of Energy, vol.87, no.1, pp.72-75.

Saxena, R.C., Adhikari, D.K. and Goyal, H.B., (2009); Biomass-Based Energy Fuel Cell through Biochemical Routes, Renew. Sust. Energ. Rev. Vol.13, pp.167-178.

Rubin, E.M., (2008); Genomics of Cellulosic Biofuels, Nature, vol.454, pp.841-845.

Sugano, Y., and Tamiya, E., (2009); A direct Cellulose-Based Fuel Cell System, Journal of Fuel Cell Technology, vol.9, no.1, pp.114-119.

Bialasiewicz, J.T., (2008); Renewable Energy Systems with Photovoltaic Power generations: Operation and Modeling, IEEE Trans. on Industrial Electronics, vol.55, no.7, pp.2752-2758.

Okabe, M., Nakazawa, K., Taruya, K., and Handa, K., (2008); Verification test of solar-powered hydrogen station (SHS) with photovoltaic modules, Honda R&D Technical Review, Vol.20, No.1, pp.67-73.

Ramos-Paja, C.A., Bordons, C., Romero, A., Giral, R., and Martinez-Salamero, L., (2009); Minimum Fuel Cell Consumption Strategy for PEM Fuel Cell, Trans. on Industrial Electronics, vol.56, no.3, pp.685-696.

KE Jin, Xinbo Ruan, MengxiongYang, and Min Xu, (2009); A Hybrid Fuel Cell Power System, Trans on Industrial Electronics, vol.56, no.4, pp.1212-1222.

Tabo, E., Kuzuoka, K., Takada, M., and Yoshida, H., (2004); Fuel cell vehicle technology trends and MMC initiatives, Mitsubishi Motors Technical Review, No.16, pp.51-55.

Kotz, R., Muller, S., Bartschi, M., Schnyder, B., Dietrich, P., Buchi, F.N., Tsukada, A., Scherer, G., Rodatz, P., Garcia, O., Barrade, P., Hermann, V., and Gallay, R., (2001); Supercapacitors for peak-power demand in fuell-cell-driven cars, Electrochemical Society Proceedings, Vol.2001-21, pp.564-575.

Rodatz, P., Garcia, O., Guzzella, L., Buchi, F., Bartschi, M., Tsukada, A., Dietrich, P., Kotz, R., Scherer, and G., Wokaun, A., (2001); Performance and operation characteristics of a hybrid vehicle powered by fuel cells and supercapacitors, Soc. of Automotive Eng. 2003 Congress, SAE Paper 2003-01-0418, pp.1-12.

Konishi, H., Akizuki, M., Ogawa, T., Kojima, H., Yamada, Y., Fujii, H., Matsunaga, N,. Yoshida, Y., Ishida, T., nad Warashina, T., (2008); Development of a Solar and Fuel Cell Powered Hybrid Electrical Vehicle Cocoon 2007, Proc. of 2008 JSME Conf. on Robotics and Mechatronics, 2P1-A18, pp.1-4.

Obara, H., (2004); Progress of Development on the Hybrid Solar Car in Tamagawa University, Journal of Fuel Cell Technology, vol.4, no.2, pp.103-107.

Nishimura, I., (2008); Design and Fabrication of Fuel Cell Vehicle Regarding Manufacturing Education, Proc. of 2008 JSME Conf. on Robotics and Mechatronics, 2P1-A13, pp.1-4.

Takahashi, Y., (2009a); Ultra Light Weight Fuel Cell Electrical Vehicle (UL-FCV), Proc. of IEEE Int. Symp. on Industrial Electronics, pp.189-194.

Takahashi, Y., (2009b); Environmental System Education using Small Fuel Cell Electrical Vehicle, Journal of Fuel Cell Technology, vol.9, no.1, pp.128-131.

Yamamuro, S., (2003); Development of Fuel Cell Powered Wheelchair, Kuromoto Kihou, no.52, pp.40-44.


**Solar Energy**

Edited by Radu D Rugescu

ISBN 978-953-307-052-0
Hard cover, 432 pages
**Publisher** InTech
**Published online** 01, February, 2010
**Published in print edition** February, 2010

The present “Solar Energy” science book hopefully opens a series of other first-hand texts in new technologies with practical impact and subsequent interest. They might include the ecological combustion of fossil fuels, space technology in the benefit of local and remote communities, new trends in the development of secure Internet Communications on an interplanetary scale, new breakthroughs in the propulsion technology and others. The editors will be pleased to see that the present book is open to debate and they will wait for the readers’ reaction with great interest. Critics and proposals will be equally welcomed.